



A logic-tree based probabilistic seismic hazard assessment for the central ionian islands of cephalonia and ithaca (Western Greece)

George Kaviris · Angelos Zymvragakis · Vasilis Kapetanidis · Vasiliki Kouskouna · Ioannis Spingos · Nikolaos Sakellariou · Nicholas Voulgaris

Received: 26 February 2024 / Accepted: 28 August 2024
© The Author(s), under exclusive licence to Springer Nature B.V. 2024

Abstract The Central Ionian Islands of Cephalonia and Ithaca belong to the most seismically active Greek region, mainly due to the presence of the dextral Cephalonia-Lefkada Transform Fault Zone. The study area has experienced strong earthquakes in the twentieth century, including the destructive 1953 sequence with maximum intensity 9.0. The Paliki peninsula, western Cephalonia, hosted two strong earthquakes ($M_w = 6.1$ and 5.8) in 2014, with ground acceleration reaching ~ 560 cm/s² and 735 cm/s², respectively. This study updates the seismic hazard evaluation in Cephalonia and Ithaca using new data and computational techniques to reduce epistemic uncertainties. The probabilistic approach of Cornell and McGuire was used, and the uncertainties are reduced through data variability of the source models, seismicity data, and Ground Motion Prediction Equations using a logic tree approach, sampled by implementing the Latin Hypercube Sampling method. The spatial distribution of Peak Ground Acceleration and Peak Ground Velocity for return periods of 475 and

950 years indicates low variation in the entire study area and that the Paliki peninsula possesses the highest level of seismic hazard. Additionally, site-specific analysis across the three main towns, Lixouri and Argostoli in Cephalonia and Vathi in Ithaca, reveals that Lixouri has the highest level of seismic hazard, while Vathi the lowest.

Keywords Probabilistic seismic hazard · Ground motion parameters · Logic tree · Epistemic uncertainty

1 Introduction

The Ionian Islands, in Western Greece, are widely recognized as an area of high seismic activity and are among the most seismically active regions in Europe. Specifically, the Central Ionian Islands (Fig. 1) stand out as the most seismically hazardous area in Greece (EAK 2003). Cephalonia Island, in particular, has hosted two $M_w \geq 6.7$ earthquakes (Makropoulos et al. 2012) within a 30-year span. Therefore there is an obvious need of a new seismic hazard assessment with updated seismicity data and sophisticated statistical techniques to reduce epistemic uncertainty, performed with modern software, is crucial for urban planning to mitigate seismic risk.

Seismic hazard is dedicated to investigating the phenomena triggered by earthquakes, with ground motion being the most significant as it acts as catalyst

Supplementary Information The online version contains supplementary material available at <https://doi.org/10.1007/s10950-024-10242-3>.

G. Kaviris (✉) · A. Zymvragakis · V. Kapetanidis · V. Kouskouna · I. Spingos · N. Sakellariou · N. Voulgaris
Department of Geophysics and Geothermics, National and Kapodistrian University of Athens (NKUA),
Panepistimiopolis, Zografou, 15784 Athens, Greece
e-mail: gkaviris@geol.uoa.gr

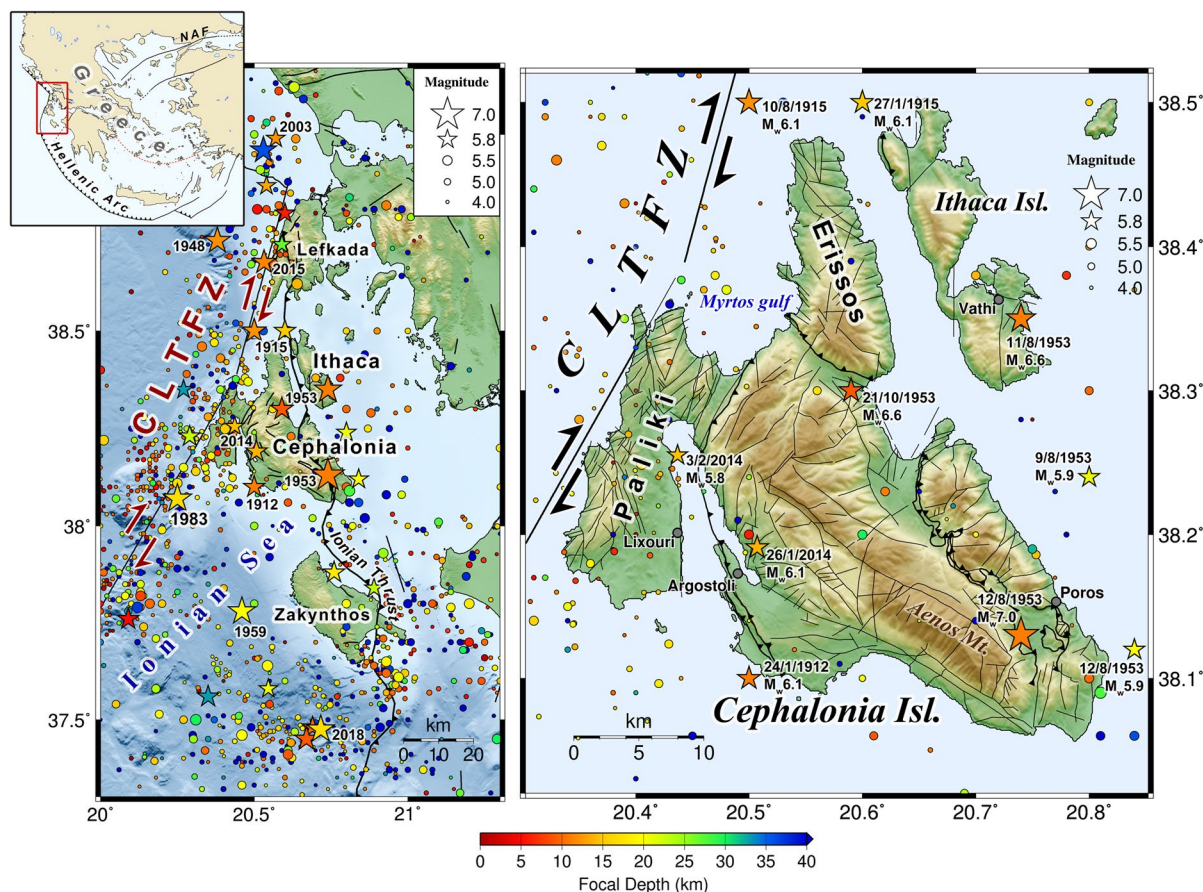


Fig. 1 Map of the Central Ionian Islands in Western Greece (red rectangle in the inset map of Greece), presenting the seismicity catalogue of Makropoulos et al. (2012), covering the period 1900–2009, extended up to 2019 (this study). (Right) Close-up of the Cephalonia and Ithaca Islands. Earthquakes with $M_w \geq 5.8$ are presented as stars. The dates and magnitudes

of significant earthquakes of the period 1900–2019 are marked on the map. The simple fault lines are from the NOAFAULTS v5.0 database (Ganas et al. 2013a; Ganas 2023). Barbed bold lines indicate thrust faults (Lekkas et al. 2001; Pérouse et al. 2017). CLTFZ: Cephalonia-Lefkada Transform Fault Zone; NAF: North Anatolian Fault

for potential secondary catastrophic events like rock-falls and liquefaction (Wang 2005). To assess seismic hazard, we quantify ground motion by estimating Intensity Measurement Types (IMT), such as Peak Ground Acceleration (PGA), Peak Ground Velocity (PGV) and Spectral acceleration (S_a), through statistical methods (Gumbel and Lieblein 1954; Cornell 1968). The most common approach to compute the aforesaid parameters is the classic probabilistic method, initially proposed by Cornell (1968) and later commercialized by McGuire (1976), that introduces the usage of a seismotectonic model. Given the high seismicity of Greece, many seismic hazard assessment studies have been conducted, dating as far back

as 1985 (Makropoulos and Burton 1985) and continuing to the present (Bonatis 2020; Bonatis et al. 2021; Pavlou et al. 2021; Kaviris et al. 2022a, 2022b, 2023).

Earthquakes in the area of the Central Ionian Islands have produced high PGA values. For example, the two 2014 Cephalonia major events produced ground acceleration of about 560 cm/s^2 and 735 cm/s^2 , respectively (Kassaras et al. 2017). These values well exceed the regulations proposed by the 2003 National Building Code (EAK 2003), which is a PGA value of 0.36 g ($\sim 350 \text{ cm/s}^2$) for a return period of 475 years. Such a difference between recorded ground motion values and the regulations highlights the need for an updated seismic hazard model. To

this extent, previous studies have been conducted for Cephalonia and Ithaca, as evidenced by the work of cited researchers (Bonatis 2020; Bonatis et al. 2021; Sakkas et al. 2022). Those studies estimate a PGA range of 200–900 cm/s² for the study area. Objective of the present study, in line with Cornell’s insights, is to investigate the possibility of reducing the considerable uncertainties regarding seismogenic sources and seismic wave attenuation. The latter can be achieved by introducing a complex logic tree approach to estimate ground motions.

In this work, we assess seismic hazard by estimating PGA and PGV for Cephalonia and Ithaca, and Sa exclusively for the most populated localities of these islands, i.e. Lixouri, Argostoli, and Vathi. To mitigate uncertainties, we have developed an extensive and “non-trivial” logic tree decision diagram for estimating IMT. In addition, we adopt a stochastic statistical sampling method to capture a substantial portion of the Probability Density Function (PDF) for each IMT. By executing these techniques, the goal of this study is to effectively reduce the prevailing uncertainties and establish an accurate seismic hazard model that will have the potential to be applied in more precise seismic risk assessments for this highly seismically active study area. The incorporation of the complex logic tree approach, combined with stochastic sampling techniques, has resulted in a seismic hazard model that significantly reduces epistemic uncertainties. This is particularly crucial given the high seismicity of the study area.

2 Seismotectonic setting and historical background

The heightened seismic activity in the area of the Central Ionian Islands is mainly attributed to the presence of the Cephalonia-Lefkada Transform Fault Zone (CLTFZ), a dextral plate boundary trending SSW-NNE (Fig. 1). This fault zone bounds the western coasts of Cephalonia and Lefkada Islands and intersects with a complex network of onshore active faults. The CLTFZ, roughly outlined by the SSW-NNE alignment of the earthquake epicenters, serves as a link between the NW-SE-trending major features of the Hellenic Arc in the south, and the collision front of the Apulian platform with the Hellenic foreland in the north. This configuration creates a

shear zone of intense deformation, leading to major earthquakes that have caused substantial damage and loss of life in the recent past, particularly on Cephalonia and Ithaca Islands. The CLTFZ exhibits a strike of ~N15°E on the latitude of Lefkada Island, while further to the south, its trend shifts to ~N30°E as it passes offshore Cephalonia (Fig. 1). The northern right-lateral Lefkada segment that lies between the NW offshore part of Lefkada and the northern offshore part of Cephalonia is 40 km long and ESE-dipping (Underhill 1989; Louvari et al. 1999). The southern Cephalonia segment, located close to the western offshore part of Cephalonia, is 90 km long and has similar geometry and kinematic properties to the Lefkada segment, as proven by geological and tectonic data (Sachpazi et al. 2000; Kokinou et al. 2006). The two slightly offset segments of the CLTFZ interact within Myrtilos Gulf at northern Cephalonia, likely forming a transfer zone of extensional step-overs (Karakostas et al. 2015). The regional crustal stress field promotes strike-slip faulting (Kapetanidis and Kassaras 2019), but the convergence of the African plate with the Aegean microplate introduces compression in a WSW-ENE direction. Differential GPS measurements have revealed a clockwise rotation of Cephalonia Island, relative to a station located on Aenos mountain, with the largest values observed at the western (Paliki) and northern (Erissos) parts of the island (Lagios et al. 2007). The broader area of Cephalonia features east-dipping NW- to NNW-striking thrust structures (Stiros et al. 1994), which may sporadically undergo seismic reactivation, resulting in earthquakes with a significant reverse dip-slip component. The Ionian Thrust traverses the southeastern part of Cephalonia Island and likely extends offshore, passing between Cephalonia and Ithaca (Underhill 1989). Additional thrust structures are observed at Aenos Mountain and Argostoli, extending northward and separating Paliki from the rest of Cephalonia.

Cephalonia has a historical record of significant earthquakes. The SHEEC catalog (Stucchi et al. 2013) and the AHEAD database (Albini et al. 2013) contain 14 historical earthquakes occurring between 1469 and 1867 with macroseismic epicenters near Lixouri and Argostoli. During the twentieth century, a significant $M_w=6.1$ earthquake occurred on 12 January 1912, south of Argostoli (Makropoulos et al. 2012; Fig. 1), killing 8 people and injuring 40 in Poros (Papazachos and Papazachou 2003). Its focal

mechanism, estimated from the directivity of macroseismic data, indicates strike-slip faulting (Papazachos et al. 1999). Another major earthquake of $M_w=6.1$ occurred on 27 January 1915 near Ithaca. It also exhibited an estimated dextral SW-NE strike-slip focal mechanism and was responsible for the collapse or extensive damage of many houses.

On 9 and 11 August 1953, two earthquakes of $M_w=5.9$ and 6.6, respectively, occurred east of Cephalonia Island, the latter with an epicenter on Ithaca Island. They were followed on 12 August by an even larger earthquake of $M_w=7.0$ at the southeastern part of Cephalonia Island, with a location error estimate of ~ 50 km (Anderson and Jackson 1987). Its focal mechanism, determined from first motion polarities, indicates reverse faulting in a NNW-SSE direction (McKenzie 1972), although estimates from macroseismic data suggest strike-slip faulting (Papazachos et al. 1999). The latter discrepancy is indicative of the significant uncertainties associated with the determination of fault parameters for earthquakes of that period, when data availability and quality was rather poor. However, in both instances, the P-axis aligns with the direction of maximum horizontal compression (Kapetanidis and Kassaras 2019), as well as with the direction of shortening ($N258^\circ E$) in the area of the Central Ionian Sea, maintaining an extension-to-shortening ratio of 1:3 (Ganas et al. 2013b). The maximum intensity value of the 1953 earthquakes at Cephalonia Island was $I_{\max}=9/10$, observed at five localities, among which Argostoli and Lixouri (Sakkas et al. 2010), however estimated even higher due to cumulative damage. The 1953 earthquake sequence, also known as the “Great Cephalonia (Ionian) earthquakes” (Kouskouna et al. 2021), being the most destructive of the modern era in Greece, occurred when no antiseismic measures were taken in the country. This sequence initiated the implementation of the first, even simple and not adequate, National Building Code, in 1959, to mitigate the risk from seismic hazards in Greece.

Another significant earthquake was an $M_w=6.7$ event that occurred on 17 January 1983, approx. 15 km southwest of Paliki. Due to its offshore epicenter, it was reportedly felt to Cephalonia Island (EMS intensity IV at Argostoli), whereas its strongest aftershock, on 23 March 1983, was more damaging (max intensity VII), as its epicenter was located further north, closer to the island. The mainshock

has been interpreted as a strike-slip rupture on a southeast-dipping fault with a relatively low angle (Papadimitriou 1988), likely with a thrust component (Scordilis et al. 1985). A similar faulting type, i.e. dextral strike-slip on an east-dipping low-angle fault, was determined for a recent major earthquake ($M_w=6.7$) that occurred southwest of Zakynthos Island on 25 October 2018 (Papadimitriou et al. 2021).

The most recent major seismic activity on Cephalonia Island comprised of an earthquake “doublet” that occurred on 26 January and 3 February 2014, with $M_w=6.1$ and 5.8, respectively, on Paliki (Papadimitriou et al. 2014; Karakostas et al. 2015; Karastathis et al. 2015; Sokos et al. 2015). Moment tensor inversions for both events support dextral strike-slip faulting on SSW-NNE-trending, steep-dipping faults, with most solutions indicating a slight tilt toward an east-dipping direction. Secondary N-S- to SW-NE-oriented surface ruptures observed at the central and northern part of Paliki peninsula after these earthquakes also indicate dextral strike-slip kinematics (Valkaniotis et al. 2014). Fault plane models, constructed using the observed co-seismic deformation, reveal that the two earthquakes occurred on two sub-parallel fault segments, in the southern and the northern parts of the Paliki peninsula, respectively (Sakkas and Lagios 2015). Coulomb stress transfer due to the 2014 earthquake “doublet” may have accelerated the occurrence of a major earthquake ($M_w=6.3$) on 17 November 2015 (Papadimitriou et al. 2017) on Lefkada (Fig. 1); an area that was already stress-loaded after the $M_w=6.3$ earthquake of 14 August 2003 (Papadimitriou et al. 2006).

The 1953 earthquake sequence on Cephalonia is among the most significant ones to have occurred in Greece during the instrumental period, leaving a profound societal imprint. The devastation was extended on the islands of Cephalonia, Ithaca, and Zakynthos, resulting in the destruction of $\sim 83\%$ of the building stock. The human toll was significant, with 455 fatalities, 21 individuals reported missing and 2412 people sustaining injuries (Papazachos and Papazachou 2003). It was also the cause of a decline in the population of Cephalonia, Ithaca, and Zakynthos during the following decades, as people abandoned the islands and migrated mainly to urban centers of Greece or abroad (Mavroulis and Lekkas 2021).

3 Methodology, input data and model parameters

The PSHA results of the approach introduced by Cornell (1968) and McGuire (1976) are in the form of annual probabilities of surpassing specific random values of acceleration, velocity, or spectral acceleration. Subsequently, the final output consists of PGA, PGV, or S_a levels corresponding to the selected return period. A pioneering aspect of this methodology, at the time of its inception, was the incorporation of a source model to depict the seismotectonic attributes of each study region. These models are classified according to the knowledge of the existing active faults within a region. For instance, a model may include the actual fault sources of the study area and report the annual exceedance rates for each magnitude bin per fault. This requires a good awareness of the dynamic characteristics of each fault. On the other hand, a source area model takes the form of polygons where seismicity is distributed, following a normal distribution within each polygon, and all attributes are consistent. This model type is typically employed in regions where the occurrence rates of all potential active faults are not well documented or are unmapped. This is partly the situation in our study area, Cephalonia and Ithaca, where the majority of active faults are offshore, and their dynamic characteristics are not known in detail. Consequently, the source area type of model was adopted for this study.

The use of a single model may introduce high epistemic uncertainties regarding the seismological attributes of the broader study area. A conventional strategy for addressing epistemic uncertainties in PSHA involves introducing variability in the input data (Bommer and Scherbaum 2008; Atkinson et al. 2014; Marzocchi et al. 2015; Kaviris et al. 2023). To address this concern, we integrated three models into our computational framework, i.e., the European Seismic Hazard Model 2013 (ESHM13) by Woessner et al. (2015), its subsequent update, ESHM20, developed by Danciu et al. (2021), and the local Ionian–Island source area model formulated by Bonatis (2020), herein referred to as BON20. Visual representations of these models are available in Fig. 2a–c. ESHM13, ESHM20, and BON20 were treated as equivalent in our analysis, as each one exhibits distinct advantages and disadvantages in comparison to the others, thus preventing in designating one as superior. This decision was substantiated

by examining the surface area of each source zone within these models. Small polygons, like the ones of ESHM13 and BON20 in the Central Ionian Islands (Fig. 2a and c), provide a more precise description of the seismotectonic features within the area, whereas larger polygons, as those of ESHM20 (Fig. 2b), are less accurate in describing these features, but with a higher number of earthquakes for statistical analysis. The latter provides insight into comparing the seismicity parameters obtained for each source model. BON20 (Fig. 2c) has smaller zones providing a more accurate description of the seismotectonics of the Ionian Islands, when compared to the other two models. However, the required seismicity data of the small source areas around Cephalonia and Ithaca will result in a complex and non-smooth spatial distribution of the computed PGA and PGV values, which may hinder drawing conclusions about the seismic hazard of the study area. Consequently, implementing both local and non-local models is the best option to address this problem.

In Greece, the instrumental earthquake catalogue of Makropoulos et al. (2012) is specifically tailored for seismic hazard studies, as it has a threshold magnitude of $M_s=4.0$ and $M_w=4.1$. It covers the period from 1900 to 2009, with the significant limitation of not including earthquakes since 2010. This lack of data is noteworthy because, as mentioned in the introduction, events such as those that occurred in 2014 and 2015 would be omitted from the computational framework. To address this issue, we extended the earthquake catalogue to 2019 in a consistent manner, following the same methodology as Makropoulos et al. (2012), i.e. incorporating reviewed events from the Bulletin of the International Seismological Centre (ISC). A common practice in PSHA is to decluster earthquake catalogues in order to retain only the parent earthquakes, removing foreshocks and aftershocks. However, this practice is debatable, as there have been reports suggesting that aftershocks can generate significant ground motions and are often responsible for additional damage (Marzocchi and Taroni 2014; Taroni and Akinci 2021). In this study, we opted not to decluster the earthquake catalogue, as this would result in loss of valuable data, especially considering that Cephalonia and Ithaca are regions characterized by frequent earthquake sequences.

The seismicity parameters of each source area required for PSHA encompass the magnitude of

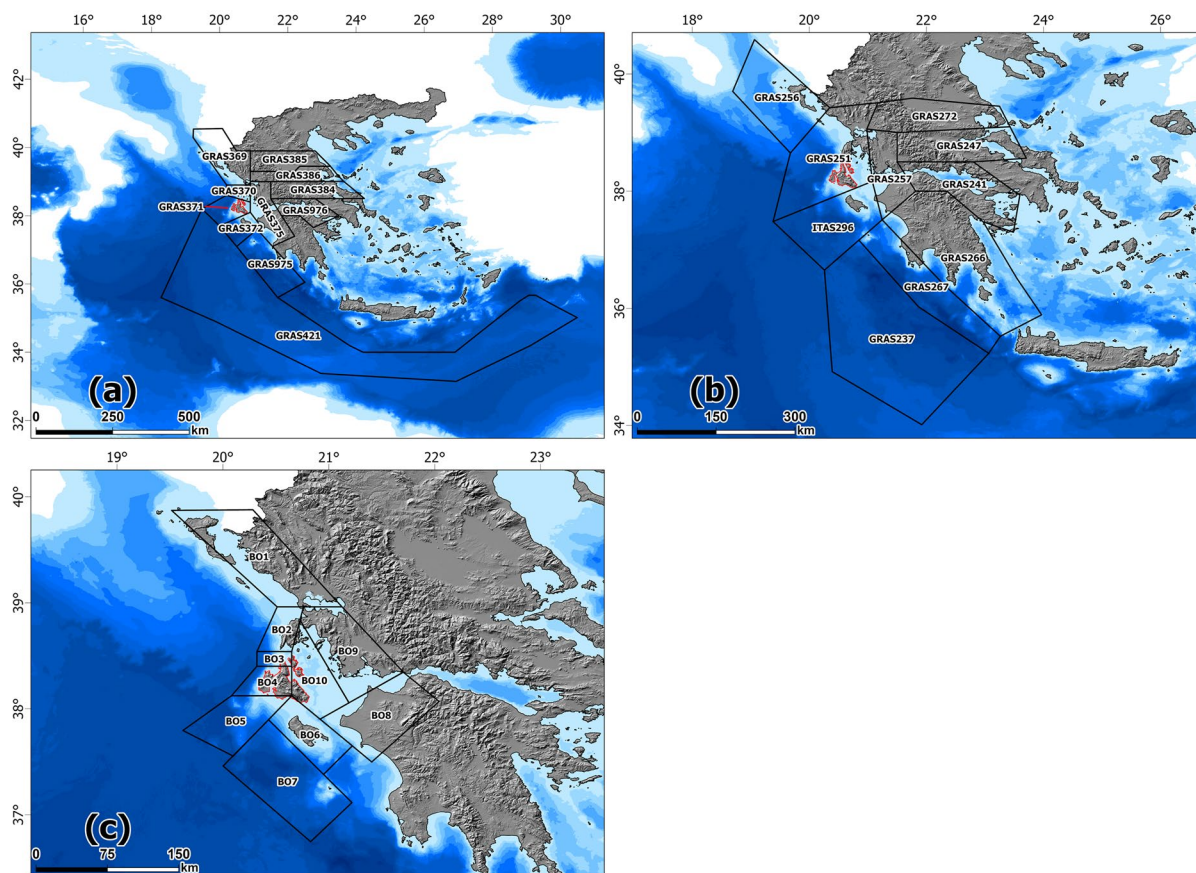


Fig. 2 The three source area models employed in this study: (a) ESHM13 (Woessner et al. 2015), (b) ESHM20 (Danciu et al. 2021), and (c) BON20 (Bonatis 2020). To determine the

source areas from ESHM13 and ESHM20 contributing to the ground motions in Cephalonia and Ithaca, a selection distance of 100 km was applied (Kaviris et al. 2022a, 2022b, 2023)

completeness (M_c), the annual rate of M_c exceedance (λM_c), the maximum expected magnitude (M_u), and the b -value of the Gutenberg–Richter Frequency–Magnitude Distribution (FMD) (Gutenberg and Richter 1944). We herein employ two methods for calculating M_c and the b -value. The first is the classical maximum curvature method (MAXC), which was originally introduced by Wiemer and Wyss (2000) and identifies M_c by pinpointing the maximum curvature of the FMD curve through the calculation of its first derivative's highest value. Subsequently, the b -value is determined using the maximum likelihood method introduced by Aki (1965). Overall, MAXC is highly reliable and robust and has undergone validation in several PSHA studies (Zhou et al. 2018; Pavlou et al. 2021; Kaviris et al. 2023). The second method, proposed by Godano and

Petrillo (2023), offers a rapid and straightforward estimation of M_c . It relies on the observation that the Gutenberg–Richter distribution exhibits an exponential behavior for magnitudes exceeding M_c and a linear behavior for the smaller ones. Consequently, the average magnitude value (M_a) exhibits linear increase as the threshold magnitude (M_{th}) increases and the deviations from this behavior allow for an accurate M_c computation, while the linearity of M_a versus M_{th} facilitates the b -value estimation. In this study, we seize the opportunity to also explore this new method for M_c and b -value estimation, aiming to comprehend its advantages and limitations for future assessments. Variability was also considered for the M_u parameter, because of the absence of a definitive estimation technique. Specifically, three techniques are utilized to estimate M_u : the first, yielding the lowest possible

M_u , is based on the maximum observed earthquake magnitude ($M_{\max\text{obs}}$) within each source area. An intermediate M_u value is estimated through the Robson–Whitlock–Cooke (RWC) technique, as described by Robson and Whitlock (1964) and Cooke (1979). RWC introduces a small positive factor based on the second maximum earthquake magnitude ($M_{\max n-1}$). The highest potential M_u is determined by adding the positive factor 0.5 to $M_{\max\text{obs}}$. Finally, λM_c is computed using the maximum likelihood estimator technique outlined in the works of Kijko and Sellevoll (1989) and Kijko and Smit (2012). Summarizing, a strong variability has been included regarding the adoption of source models and the calculation of seismicity parameters.

The Ground Motion Prediction Equation (GMPE) plays a pivotal role in PSHA by providing estimations of peak ground motions that take into account the earthquake magnitude, distance from the site, focal mechanism type, and soil conditions. It is important to emphasize that the prediction of ground motions resulting from an earthquake may introduce errors, especially in the near-field, hence GMPEs are empirical relationships that possess notable epistemic uncertainties. In this context, variability is a critical aspect, allowing us to incorporate a range of PGA, PGV, and Sa values for the same independent variables, such as earthquake magnitude and distance. In our study, we employed GMPEs that have undergone rigorous testing, validation, and ranking in recent PSHA studies (Pavlou et al. 2021; Kaviris et al. 2022a, 2022b, 2023; Sakkas et al. 2022). For PGA, we utilized the GMPEs proposed by Skarlatoudis et al. (2003) [SKA03], Danciu and Tselentis (2007) [DAT07], Sakkas (2016) [SAK16] and Chousianitis et al. (2018) [CHO18]. For PGV, the GMPEs of Skarlatoudis et al. (2007) [SKA07], Danciu and Tselentis (2007) [DAT07] and Chousianitis et al. (2018) [CHO18] were selected and for Sa the GMPE of Danciu and Tselentis (2007) [DAT07] was chosen. For PSHA purposes, it is essential not to assign to the mentioned GMPEs only one type of focal mechanism (normal or non-normal) to each source area, which can lead to overestimation or underestimation of peak ground motions. To address this challenge, we utilized the focal mechanism catalogue proposed by Kapetanidis and Kassaras (2019) to determine the accurate percentages of normal and non-normal focal mechanisms for each source area. We then applied those percents to the selected

GMPEs to ensure accurate proportions between the normal and non-normal versions of each GMPE. This approach allows to avoid the need for interpolating the type of focal mechanism for each source area. The percentages can be found in Table S1. The seismicity data of the source areas of each seismotectonic model that contain Cephalonia and Ithaca is presented in Table 1.

The concept of logic tree diagrams, originally introduced by Kulkarni et al. (1984), has consistently proven to be a reliable method for mitigating uncertainties (Bommer and Scherbaum 2008; Atkinson et al. 2014; Marzocchi et al. 2015). In PSHA, a logic tree comprises multiple branches, each representing a potential seismic hazard outcome, reflecting the associated uncertainties. These branches are created to account for different choices that the analyst deems feasible and, to express the level of confidence in each one, every branch is assigned a normalized weight. Within the context of this paper, the logic tree visually represents the steps discussed (Fig. 3). The process commences with the source models, where three branches are established, one for each model, with equal weighting. Subsequently, for every source area of each source model, additional branches are introduced to accommodate variables, such as b-values, M_c , and $\lambda(M_c)$, determined using the MAXC technique and the newly proposed method by Godano and Petrillo (2023). Moreover, variations in M_u are considered by incorporating three branches, representing low, intermediate, and high M_u levels. Furthermore, the selected GMPEs are integrated into the analysis, each one associated with a minor logic tree that accounts for the percentages of normal and non-normal focal mechanism types within each source area. It is important to note that this complexity refers to a single source area only. Consequently, the total number of logic tree samples becomes extraordinarily large, akin to the situation in PSHA for Canada (Kolaj et al. 2020). In such cases, it is essential to implement statistical sampling methods, as emphasized by Pagani et al. (2014). For our specific needs, the Latin Hypercube Sampling (LHS) method, initially proposed by McKay et al. (1979), is deemed the most suitable. Unlike the random sampling of the Monte Carlo technique, LHS divides the input ranges into equal intervals, ensuring that only one value is selected from each interval. This approach offers a more systematic and representative way to sample

Table 1 Seismicity data of the zones that include the study area. N-FM (%) and NN-FM (%) are the percentages of Normal and Non-Normal focal mechanisms. M_{maxobs} is the maximum observed M_w , M_{urRWC} is the maximum expected magnitude using the RWC method and $M_{maxobs+0.5}$ is the maximum observed magnitude plus a positive factor of 0.5. M_{cGP23} , b-value_{GP23} and $\lambda(M_{cGP23})$ are the magnitude of completeness, the b-value and the annual rate of M_c , all computed using the method of Godano and Petrillo (2023). The same pattern is used for the MAXC method in the symbols M_{cMAXC} , b-value_{MAXC}, b-value_{MAXC} and $\lambda(M_{cMAXC})$

Source Area	N-FM (%)	NN-FM (%)	M_{maxobs}	M_{urRWC}	$M_{maxobs+0.5}$	M_{cGP23}	b-value _{GP23}	$\lambda(M_{cGP23})$	M_{cMAXC}	b-value _{MAXC}	$\lambda(M_{cMAXC})$
GRAS370 (ESHM13)	0.07	0.93	6.5	6.6	7.0	5.6	1.07	0.07	4.4	0.70	0.63
GRAS371 (ESHM13)	0.13	0.87	7.0	7.2	7.5	5.1	1.10	0.64	4.1	0.92	4.88
GRAS251 (ESHM20)	0.13	0.87	7.0	7.2	7.5	5.1	1.15	1.04	4.1	0.84	7.03
BO3 (BON20)	0.15	0.85	6.3	6.4	6.8	5.5	1.08	0.05	4.1	0.64	0.29
BO4 (BON20)	0.09	0.92	6.2	6.2	6.7	5.0	1.10	0.23	4.1	0.93	1.48
BO10 (BON20)	0.13	0.87	7.0	7.2	7.5	6.4	1.00	0.02	4.6	0.96	0.59

the various branches of the logic tree, thereby capturing the full range of scenarios. The number of samples used for the sampling process was determined through a trial-and-error approach, yielding stable results for PGA, PGV and Sa. It was decided that 10,000 samples would be employed, consistent with the procedure followed in ESHM13 and ESHM20. PGA, PGV, and Sa values were computed using the OpenQuake engine (version 3.15.0) proposed by Pagani et al. (2014). The information regarding the configuration file that was used for these computations is available as a word file in the Supplementary material.

4 Results

The results are presented in the form of PGA and PGV spatial distribution maps for Cephalonia and Ithaca (Figs. 4 and 5, respectively), considering return periods of 475 (Figs. 4a and 5a) and 950 years (Figs. 4b and 5b). Additionally, PGA-hazard curves were generated for the three most densely populated towns in our study area: Lixouri, Argostoli, and Vathi (Fig. 6a). Those were produced to demonstrate PGA values for a wide range of return periods. Moreover, for the same sites, Uniform Hazard Spectra (UHS) were constructed by utilizing Sa levels, which correspond to their natural periods (Fig. 6b).

Based on the spatial distribution of both PGA and PGV for return periods of 475 and 950 years, the lowest values are observed in the southeastern portion of the study area. As we move towards the north and west, the values increase, reaching their peak mainly in Paliki and a small area east of the Myrtos Gulf. The pattern observed may be attributed mainly to the small distance of Paliki peninsula from the Cephalonia segment of the CLTFZ, characterized by high seismicity, as well as to the onshore faulting system, where the 2014 Cephalonia earthquakes occurred. The peak near Myrtos Gulf, where intermediate magnitude events have occurred due to the activation of secondary smaller structures transverse to the axis of the CLTFZ (Sakkas et al. 2022), may be aleatoric due to the small contour area.

The lowest PGA value for return period of 475 years is approximately 460 cm/s², and the highest around 580 cm/s² (Fig. 4a). The PGA range is about 120 cm/s², with the most intense variation

Fig. 3 A section of the logic tree diagram presented for the current PSHA computational method. The branches are provided in detail exclusively for the GRAS369 source area of the ESHM13 source model, specifically for the lowest Mu value. It is worth noting that the complete set of branches for GRAS369 would also include two additional branches for the intermediate and the highest Mu values, while the remainder of the logic tree remains consistent. The same decision-making process was applied uniformly across all source areas within each source model, with the only difference associated with the weights assigned to the final column, representing the percentages of Normal (N) and Non-Normal (NN) focal mechanisms. Seismicity data are presented in Table S1

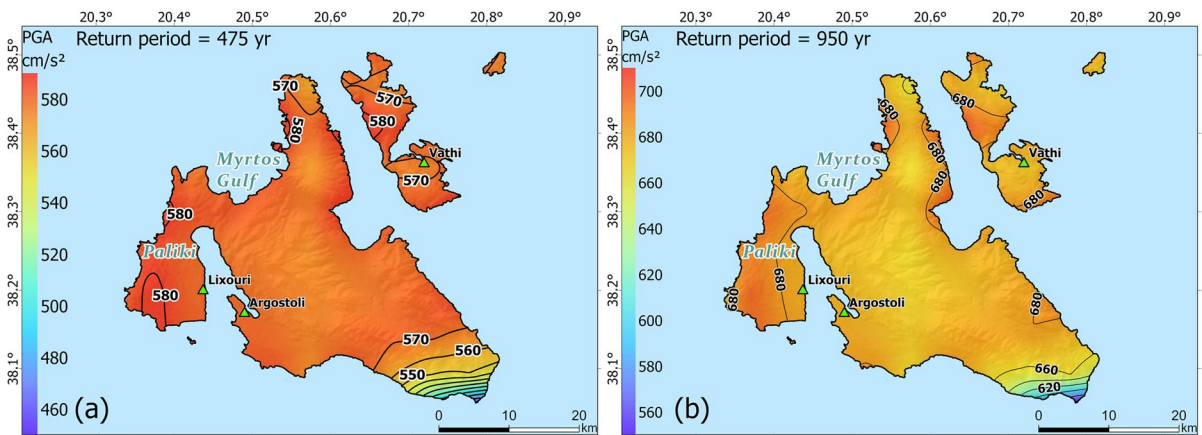
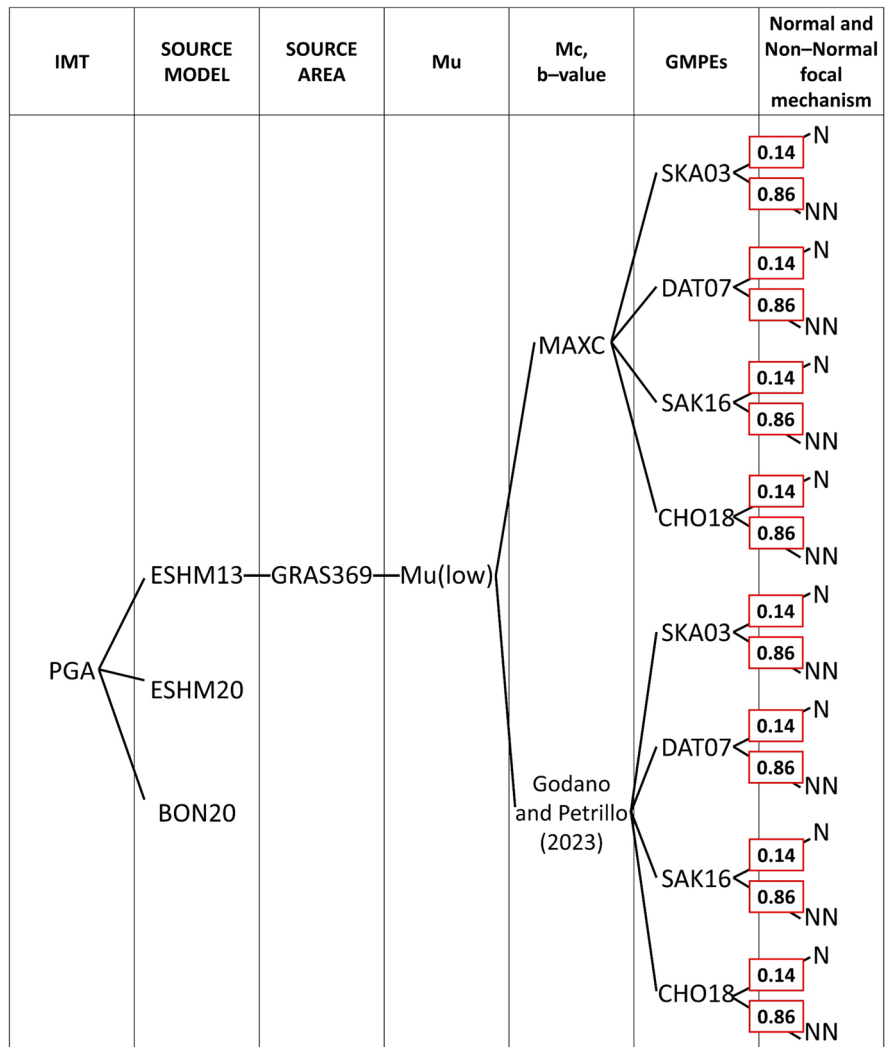


Fig. 4 PGA results for return periods 475 and 950 years (a and b, respectively)

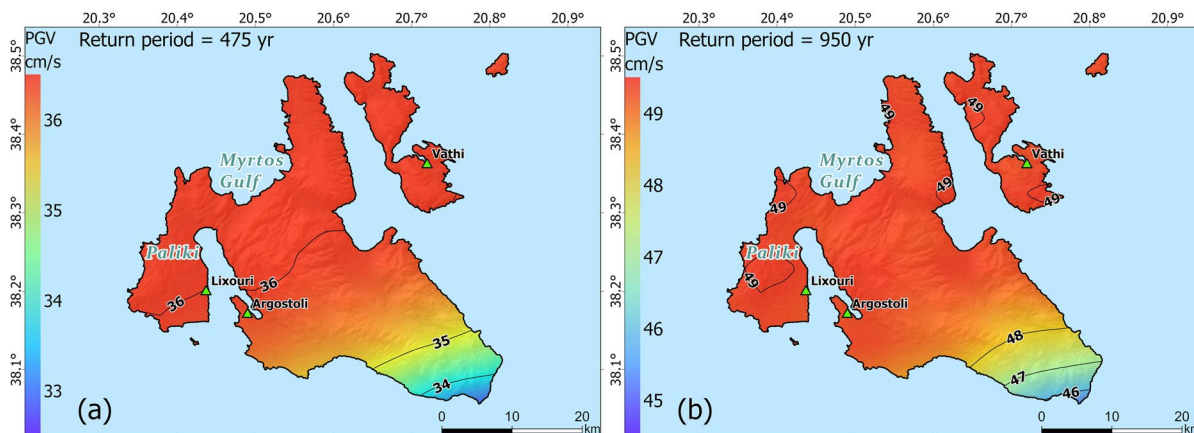


Fig. 5 PGV results for return periods of 475 and 950 years (a and b, respectively)

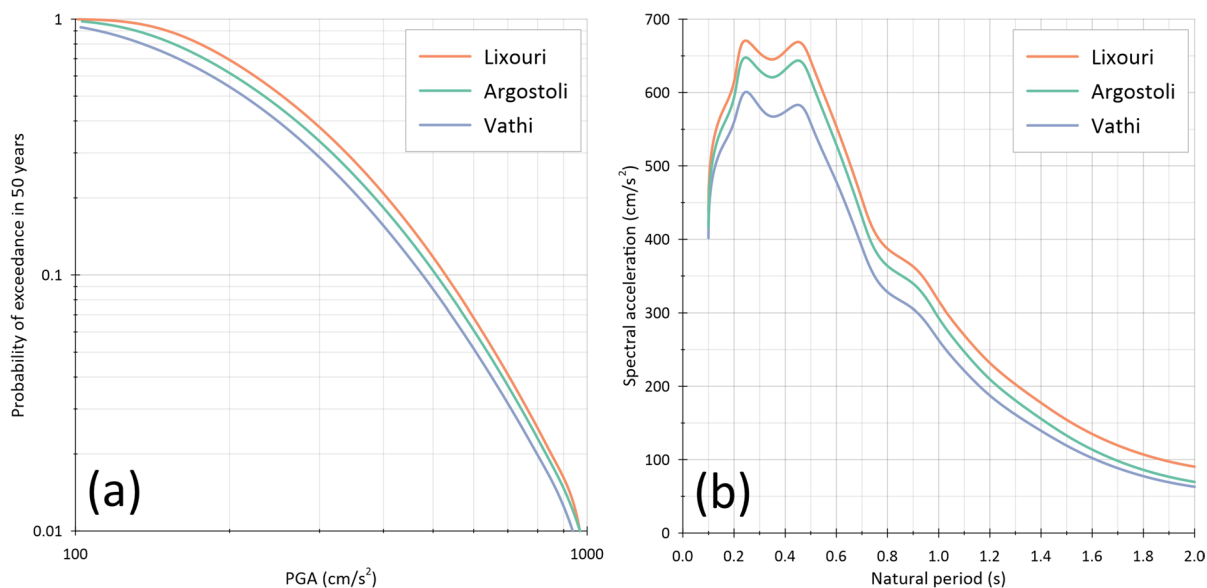


Fig. 6 PGA-hazard curves (a) and UHS in terms of Sa (b) for Lixouri, Argostoli and Vathi

occurring along the southeastern edge of Cephalonia. This indicates that intermediate to high PGA values are prevalent throughout most of the study area. Similar observations can be made for the return period of 950 years (Fig. 4b), where the difference between the highest (around 700 cm/s²) and the lowest (approximately 560 cm/s²) PGA is about 140 cm/s². Again, the high PGA variation mainly occurs along the south easternmost edge of the study area.

Regarding PGV, for a return period of 475 years (Fig. 5a), some differences can be noticed compared

to PGA. In particular, the spatial distribution is smoother, with the lowest PGV value approximately 33 cm/s, while the highest is around 36 cm/s. This relative stability in PGV values can be attributed to the smaller number of GMPEs used for PGV computation, as SAK16 does not propose a PGV model. This implies that the logic tree has significantly fewer total branches, resulting in a lower complexity of the spatial distribution. Continuing to the results of PGV for the return period of 950 years (Fig. 5b), we find a similar situation. The highest value is ~49 cm/s, and

the lowest is about 45 cm/s, with a small deviation of approximately 4 cm/s.

Continuing to the site-specific analysis and the PGA-hazard curves (Fig. 6a), we can observe the PGA levels across a range of probabilities of exceedance in 50 years. Lixouri and Argostoli exhibit similar values, with Lixouri's curve being slightly higher than that of Argostoli by approximately 10 cm/s² for all probabilities of exceedance. This small difference can possibly be attributed to their distance from the CLTFZ, as Lixouri is closer to the fault than Argostoli. Vathi displays the lowest hazard curve, which aligns with the spatial distribution of PGA values for both return periods, as Vathi is situated in a region characterized by intermediate PGA values. It is worth noting that even for the highest presented return periods, ground motions do not exceed 1 g.

Regarding the UHS for the same towns (Fig. 6b), Lixouri exhibits the highest S_a levels compared to Argostoli and Vathi across the entire range of natural periods. This observation is in agreement with the previously mentioned results. Furthermore, the UHS provides information about the natural period of the single-degree freedom system that experiences the highest S_a value, which in our case is 0.25 s. However, it is essential to acknowledge a slightly lower peak at 0.45 s, which should be considered, especially for Lixouri which experiences S_a values that are nearly identical for these two periods.

5 Discussion

The primary objective of this study is to conduct a reassessment of seismic hazard in Cephalonia and Ithaca by involving the integration of new statistical techniques aimed at reducing epistemic uncertainties related to source models, seismicity data and GMPEs. The first set of results pertains to the spatial distribution of PGA and PGV for return periods 475 and 950 years across Cephalonia and Ithaca and the second one focuses exclusively on the three most densely populated localities, namely Lixouri, Argostoli, and Vathi. For these towns, PGA hazard curves and UHS were developed to illustrate the variation in PGA values over a wide range of probabilities of exceedance and the S_a distribution across various natural periods, respectively.

The study suggests that the area of higher seismic hazard is the Paliki peninsula in western Cephalonia. This is mainly due to the vicinity of Paliki to the Cephalonia segment of the CLTFZ, maybe the most seismically active structure in Greece. In addition, high PGA values in Paliki are also influenced by the onshore local faults related with the 2014 Cephalonia earthquakes ($M_w=6.1$ and $M_w=5.8$), which also caused local ground deformation (Sakkas et al. 2022). Moreover, the area east of Myrtos Gulf has a high level of seismic hazard, although this finding may contain a considerable level of uncertainty. In the work of Sakkas et al. (2022), it was demonstrated that the post-seismic activity of the 2014 earthquake sequence primarily migrated northward, with clusters also located within the Myrtos Gulf. The site-specific results show that Lixouri has the highest PGA hazard curve and UHS, while Argostoli has intermediate curves, similar with those of Lixouri. In contrast, Vathi has the lowest maximum expected ground motions among the towns. Lixouri's proximity to the CLTFZ, in comparison to Argostoli and Vathi, may be the reason for this distribution.

The findings for both return periods offer valuable insights for structural design and engineering purposes, as more accurate local vulnerability curves can be obtained. The latter can lead to a more accurate seismic risk assessment of the area that can guide seismic retrofitting efforts, ensuring that they meet safety standards. The outcomes of the site-specific analysis for the three towns offer valuable insights into the anticipated maximum ground motions over a 50-year timeframe, taking into account varying probabilities of occurrence. Additionally, these findings help in identifying measures to prevent resonance phenomena linked to the prevailing soil period (which was at 0.25 s).

As previously mentioned, there have been several studies conducted to assess seismic hazard in Cephalonia and Ithaca. The one of Bonatis (2020) employed the same PSHA methodology as the one outlined here. However, differences exist between the source models and GMPEs used in the herein proposed PSHA. Specifically, Bonatis (2020) utilized a single seismotectonic model, BON20, and calculated PGA for a 475-year return period using various GMPEs, which, however, were not combined through a logic tree technique. The PGA results ranged from 200 to 900 cm/s², while the herein obtained values are in a

much narrower range. Nonetheless, the spatial distribution of PGA remained consistent, particularly regarding the high variability observed at the southern edge of Cephalonia. In this case, the PGA values ranged from 50 to 450 cm/s², and PGV from 0 to 25 cm/s. However, it is important to note that these results cannot be directly compared to those of the current study, given the fundamental differences in the methodologies employed. In their recent work, Sakkas et al. (2022) used the ESHM13 source model and the GMPE developed by Danciu and Tselentis (2007), only for non-normal focal mechanisms. The MAXC method was used to obtain their seismicity parameters. Therefore, due to differences in the pre-processing part, variations in the results are expected between their work and this study. The logic tree used by Sakkas et al. (2022) had significantly fewer branches compared to the one used in this PSHA, resulting in a more smoothed spatial distribution of PGA. In their computational grid, Sakkas et al. (2022) included all the Ionian Islands. Therefore, for visualization clarity, the values in Cephalonia and Ithaca are depicted as a single value of approximately 500 cm/s² for a return period of 475 years (Table 2).

The present PSHA has lower epistemic uncertainty when compared to the aforementioned studies. Additionally, a side-task was to test the new technique for the estimation of M_c and b -value, proposed by Godano and Petrillo (2023). A drawback of this method is the overestimation of M_c values when compared to other techniques (for instance, the MAXC that was also utilized in this study). The generation of high M_c values could potentially result in a limited number of data points for the estimation of the b -value, thereby leading to higher uncertainty in the regression model. The lack of a reliable b -value is a considerable drawback, given its crucial role in characterizing the seismicity for each source area. Nevertheless, the technique of Godano and Petrillo (2023) can be chosen in regions of high seismicity, where an adequate number of earthquakes certainly

exists. Consequently, this method can be selected for the region of Cephalonia and Ithaca. Given the high degree of uncertainty regarding the M_u , we chose to designate three levels for each source area (low, intermediate, and high) in order to capture a broad range of seismic hazard outcomes related to this aspect. Furthermore, by incorporating precise weights into both the normal and non-normal versions of each GMPE at each source zone, we were able to manage the uncertainty related to the extrapolation of the focal mechanism. This is a critical step in preventing the overestimation and underestimation of the maximum expected ground motions. It is worth noting that a reliable sampling technique was required for this extensive logic tree. The LHS was chosen due to its non-memoryless nature, which is particularly significant in this context, as it effectively samples a considerable portion of the entire distribution of logic tree branches.

This PSHA has certain limitations, for instance, it does not account for soil conditions, which can influence the results through amplification or attenuation phenomena. In the absence of information on true soil conditions, the study of Allen and Wald (2009), which relies only on topographic data can be used as a proxy for seismic site conditions, but it was not chosen for this PSHA in order to avoid additional potential uncertainties. Another limitation is the absence of a GMPE ranking system in the analysis, as it could provide valuable insights into which one of the selected empirical models best matches the recorded strong motion values and their relative weights for inclusion in the logic tree approach. However, it is worth noting that a recent study by Kaviris et al. (2023) conducted a GMPE ranking system for the same GMPEs as those selected in the herein computational framework, and the results indicated that the relative weights were very close to each other. This suggests that the PGA, PGV and S_a obtained here may not significantly differ from those generated using a non-equal-weighted logic tree approach.

Table 2 Comparison of the range of PGA values for Cephalonia and Ithaca among the studies by Bonatis (2020), Sakkas et al. (2022), and this study

Seismic hazard model	Bonatis (2020)	Sakkas et al. (2022)	This study
PGA (cm/s ²)	200—900	500	460—580

6 Conclusion

The aim of this study is to re-evaluate the seismic hazard for Cephalonia and Ithaca, taking into account new data and statistical methodologies. It is recognized that seismic hazard assessment is a field

characterized by significant epistemic uncertainty (Cornell 1968). Therefore, in regions like the one of the present work, which are subject to high seismic hazard, as highlighted by the current National Building Code (EAK 2003), it is essential to update the maximum expected ground motions in order to have a reliable input for future seismic risk studies (Cornell 1968).

A well established and dependable approach to addressing epistemic uncertainty involves the use of a comprehensive logic tree decision graph. In the herein proposed PSHA, we incorporate three groups of source areas, i.e., two European and one local for Cephalonia and Ithaca. These models are considered with equal weights in the computational schemes due to the lack of specific criteria indicating one model's superiority over another. Significant attention is given to the computation of seismicity parameters, where two methods were implemented for calculating the pair of M_c and b -value, and three for estimating μ . The most critical aspect is addressing the uncertainty regarding GMPEs, as these empirical relations predict the maximum expected ground motions (PGA, PGV, and S_a). We select several GMPEs that consider the epicentral type of distance, since we do not have faults, but source areas, and the type of focal mechanism. In PSHA, it is common to extrapolate the focal mechanism type for each source area, leading to the selection of GMPEs for one specific faulting type only. In this updated PSHA, we create a sub-logic tree for each GMPE that considers the relative percentages of normal and non-normal types of focal mechanisms. When considering all possible seismic hazard outcomes, it becomes clear that the final number of branches is large, making a complete enumeration almost impossible. Therefore, we opt for a sampling of the logic tree using reliable techniques to capture a significant portion of it. Consequently, we believe that this study's results have thus far achieved the lowest degree of uncertainty.

The findings of this study are presented as spatial distributions of PGA and PGV for return periods of 475 and 950 years, along with site-specific results for Lixouri, Argostoli, and Vathi (PGA-hazard curves and UHS). The highest ground motions are observed in the western portions of Cephalonia and Ithaca, with significant variability in the southeastern edge of Cephalonia. Among the towns studied, Lixouri exhibits the highest level of seismic hazard, while Vathi the

lowest. All three towns have a dominant frequency of 0.25 s. The PGA results for the first return period can be compared to the reference value proposed by EAK (2003), which divides Greece into three seismic hazard zones, each being attributed a specific PGA for bedrock conditions. For Cephalonia and Ithaca, this reference value is approximately 360 cm/s², the highest in the country. However, the maximum PGA from our proposed PSHA model is 580 cm/s², underscoring the need to update the reference value. The results for the second return period can aid the construction of critical structures, such as medical centers. The site-specific analysis results provide insights on the estimated fundamental resonance frequency and the maximum expected spectral acceleration.

Future research endeavors could involve conducting fieldwork to capture ambient noise in three spatial dimensions at various sites. This data collection would facilitate the determination of the fundamental resonance frequency of the ground across Cephalonia and Ithaca using a spatial grid. Understanding this parameter is of great significance in earthquake engineering, as it provides valuable insights into site-specific effects. Another avenue for exploration is the development of a new GMPE that specifically predicts PGA and PGV for the vertical component of ground motion. Such information would be particularly beneficial for the construction of bridges, especially in regions with high seismic activity. Furthermore, a seismic risk assessment could be undertaken, exploiting the herein proposed PSHA as an input to determine the maximum expected ground motions.

Acknowledgements We express our gratitude to the anonymous reviewer for the constructive comments that helped improve the manuscript, as well as to the editor for providing us with the opportunity to publish this study.

Author contribution Conceptualization, G.K.; methodology G.K., A.Z. and V.K. (Vasilis Kapetanidis); software, A.Z., V.K. (Vasilis Kapetanidis) and I.S., validation, G.K., A.Z., V.K. (Vasiliki Kouskouna) and N.V.; formal analysis, G.K. and A.Z.; investigation, G.K., A.Z., V.K. (Vasilis Kapetanidis), I.S. and N.S.; resources, G.K., V.K. (Vasiliki Kouskouna) and N.V.; data curation, G.K., A.Z., V.K. (Vasilis Kapetanidis), N.S. and I.S.; writing—original draft preparation, G.K., A.Z. and V.K. (Vasilis Kapetanidis); writing—review and editing, G.K., A.Z., V.K. (Vasilis Kapetanidis), V.K. (Vasiliki Kouskouna), I.S., N.S., and N.V.; visualization, A.Z. and V.K. (Vasilis Kapetanidis); supervision, G.K., V.K. (Vasiliki Kouskouna) and N.V. All authors have read and agreed to the published version of the manuscript.

Data availability Publicly available datasets were analyzed in this study. The ESHM13 and ESHM20 area sources can be found here: <http://hazard.efehr.org/en/home/>, accessed on 10th December 2023. Regarding the earthquake catalogue, the earthquake epicenters for the period of 1900–2009 were adopted from Makropoulos et al. (2012). For the recent period (2010–2019) of the catalogue, the reviewed events from International Seismological Centre (<http://www.isc.ac.uk/iscbulletin/search/bulletin/>, accessed on 20 November 2023) were used.

References

- Aki K (1965) Maximum likelihood estimate of b in the formula $\log N = a - bM$ and its confidence limits. *Bull Earthq Res Inst* 43:237–239
- Albini P, Locati M, Rovida A, Stucchi M (2013) European Archive of Historical Earthquake Data (AHEAD). Istituto Nazionale Di Geofisica e Vulcanologia (INGV). <https://doi.org/10.6092/ingv.it-ahead>
- Allen TI, Wald DJ (2009) On the use of high-resolution topographic data as a proxy for seismic site conditions (VS30). *Bull Seismol Soc Am* 99:935–943. <https://doi.org/10.1785/0120080255>
- Anderson H, Jackson J (1987) Active tectonics of the Adriatic Region. *Geophys J Int* 91:937–983. <https://doi.org/10.1111/j.1365-246X.1987.tb01675.x>
- Atkinson GM, Bommer JJ, Abrahamson NA (2014) Alternative approaches to modeling epistemic uncertainty in ground motions in probabilistic seismic-hazard analysis. *Seismol Res Lett* 85:1141–1144. <https://doi.org/10.1785/0220140120>
- Bommer JJ, Scherbaum F (2008) The use and misuse of logic trees in probabilistic seismic hazard analysis. *Earthq Spectra* 24:997–1009. <https://doi.org/10.1193/1.2977755>
- Bonatis P, Akinci A, Karakostas V, Papadimitriou E, Kaviris G (2021) Near-fault broadband ground motion simulation applications at the Central Ionian Islands. *Greece Pure Appl Geophys* 178:3505–3527. <https://doi.org/10.1007/s00024-021-02825-9>
- Bonatis P (2020) Strong ground motion simulation in the Central Ionian Islands using a hybrid (deterministic and stochastic) approach. Master Thesis, School of Geology, Aristotle University of Thessaloniki, p 129. <https://doi.org/10.26262/heal.auth.ir.316788>
- Chousianitis K, Del Gaudio V, Pierrri P, Tselentis G-A (2018) Regional ground-motion prediction equations for amplitude-, frequency response-, and duration-based parameters for Greece. *Earthquake Engng Struct Dyn* 47:2252–2274. <https://doi.org/10.1002/eqe.3067>
- Cooke P (1979) Statistical inference for bounds of random variables. *Biometrika* 66:367–374. <https://doi.org/10.1093/biomet/66.2.367>
- Cornell C (1968) Engineering seismic risk analysis. *Bull Seismol Soc Am* 58:1583–1606
- Danciu L, Nandan S, Reyes C, Basili R, Weatherill G, Beauval C, Rovida A, Vilanova S, Sesetyan K, Bard P-Y, Cotton F, Wiemer S, Giardini D (2021) ESHM20 - EFEHR Technical Report The 2020 update of the European Seismic Hazard Model - ESHM20: Model Overview. EFEHR European Facilities of Earthquake Hazard and Risk. <https://doi.org/10.12686/A15>
- Danciu L, Tselentis G-A (2007) Engineering ground-motion parameters attenuation relationships for Greece. *Bull Seismol Soc Am* 97:162–183. <https://doi.org/10.1785/0120050087>
- EAK (2003) Greek seismic code edited by: Earthquake planning and protection organization. Greece, Athens
- Ganas A, Oikonomou IA, Tsimi C (2013a) NOAfaults: a digital database for active faults in Greece. *Geosociety* 47, 518–530. <https://doi.org/10.12681/bgsg.11079>
- Ganas A, Marinou A, Anastasiou D, Paradissis D, Papazissi K, Tzavaras P, Drakatos G (2013b) GPS-derived estimates of crustal deformation in the central and north Ionian Sea, Greece: 3-yr results from NOANET continuous network data. *J Geodyn* 67:62–71. <https://doi.org/10.1016/j.jog.2012.05.010>
- Ganas A (2023) NOAFAULTS KMZ layer Version 5.0 (V5.0). Zenodo. <https://doi.org/10.5281/zenodo.8075517>
- Godano C, Petrillo G (2023) Estimating the Completeness Magnitude m_c and the b -Values in a Snap. *Earth Space Sci* 10:e2022EA002540. <https://doi.org/10.1029/2022EA002540>
- Gumbel E, Lieblein J (1954) Statistical theory of extreme values and some practical applications: A Series of Lectures. National Bureau of Standards, US Government Printing Office, Washington, p 33
- Gutenberg B, Richter CF (1944) Frequency of earthquakes in California. *Bull Seismol Soc Am* 34:185–188
- Kapetanidis V, Kassaras I (2019) Contemporary crustal stress of the Greek region deduced from earthquake focal mechanisms. *J Geodyn* 123:55–82. <https://doi.org/10.1016/j.jog.2018.11.004>
- Karakostas V, Papadimitriou E, Mesimeri M, Gkarlaoui C, Paradisopoulou P (2015) The 2014 Kefalonia Doublet (MW6.1 and MW6.0), Central Ionian Islands, Greece: Seismotectonic Implications along the Kefalonia Transform Fault Zone. *Acta Geophys* 63:1–16. <https://doi.org/10.2478/s11600-014-0227-4>
- Karastathis VK, Mouzakiotis E, Ganas A, Papadopoulos GA (2015) High-precision relocation of seismic sequences above a dipping Moho: the case of the January–February 2014 seismic sequence on Cephalonia island (Greece). *Solid Earth* 6:173–184. <https://doi.org/10.5194/se-6-173-2015>
- Kassaras I, Papadimitriou P, Kapetanidis V, Voulgaris N (2017) Seismic site characterization at the western Cephalonia Island in the aftermath of the 2014 earthquake series. *Geo-Engineering* 8:7. <https://doi.org/10.1186/s40703-017-0045-z>
- Kaviris G, Zymvragakis A, Bonatis P, Kapetanidis V, Voulgaris N (2022a) Probabilistic and scenario-based seismic hazard assessment on the Western Gulf of Corinth (Central Greece). *Appl Sci* 12, 11152. <https://doi.org/10.3390/app122111152>
- Kaviris G, Zymvragakis A, Bonatis P, Sakkas G, Kouskouna V, Voulgaris N (2022b) Probabilistic seismic hazard assessment for the broader messinia (SW Greece) Region. *Pure*

- Appl Geophys 179:551–567. <https://doi.org/10.1007/s00024-022-02950-z>
- Kaviris G, Zymvragakis A, Bonatis P, Kapetanidis V, Spingos I, Mavroulis S, Kotsi E, Lekkas E, Voulgaris N (2023) A Logic-Tree Approach for Probabilistic Seismic Hazard Assessment in the Administrative Region of Attica (Greece). *Appl Sci* 13, 7553. <https://doi.org/10.3390/app13137553>
- Kijko A, Sellevoll MA (1989) Estimation of earthquake hazard parameters from incomplete data files. Part I. Utilization of extreme and complete catalogs with different threshold magnitudes. *Bull Seismol Soc Am* 79:645–654. <https://doi.org/10.1785/BSSA0790030645>
- Kijko A, Smit A (2012) Extension of the aki-utsu b-value estimator for incomplete catalogs. *Bull Seismol Soc Am* 102:1283–1287. <https://doi.org/10.1785/0120110226>
- Kokinou E, Kamberis E, Vafidis A, Monopolis D, Ananiadis G, Zelilidis A (2006) Deep seismic reflection data from offshore western Greece: A new crustal model for the Ionian Sea. *J Pet Geol* 28:185–202. <https://doi.org/10.1111/j.1747-5457.2005.tb00079.x>
- Kolaj M, Adams J, Halchuk S (2020) The 6th generation seismic hazard model of Canada. In: 17th World Conference on Earthquake Engineering. pp 1–12
- Kouskouna V, Sakkas G, Cecic I, Tsimpidaros VI, Sakkas S, Kaviris G, Tertulliani A (2021) Earthquake induced crises: game tree approached risk communication and lessons learnt. *Annals Geophys* 64(3), SE329. <https://doi.org/10.4401/ag-8405>
- Kulkarni R, Youngs R, Coppersmith K (1984) Assessment of confidence intervals for results of seismic hazard analysis. In: Proceedings of the Eighth World Conference on Earthquake Engineering. San Francisco, pp 263–270
- Lagios E, Sakkas V, Papadimitriou P, Parcharidis I, Damiata BN, Chousianitis K, Vassilopoulou S (2007) Crustal deformation in the Central Ionian Islands (Greece): Results from DGPS and DInSAR analyses (1995–2006). *Tectonophysics* 444:119–145. <https://doi.org/10.1016/j.tecto.2007.08.018>
- Lekkas EL, Mavroulis SD (2016) Fault zones ruptured during the early 2014 Cephalonia Island (Ionian Sea, Western Greece) earthquakes (January 26 and February 3, Mw 6.0) based on the associated co-seismic surface ruptures. *J Seismol* 20:63–78. <https://doi.org/10.1007/s10950-015-9510-3>
- Lekkas E, Danamos G, Mavrikas G (2001) Geological structure and evolution of Cephalonia and Ithaki Islands. *Bull Geol Soc Greece XXXIV* 1:11–17
- Louvari E, Kiratzi AA, Papazachos BC (1999) The Cephalonia Transform Fault and its extension to western Lefkada Island (Greece). *Tectonophysics* 308:223–236. [https://doi.org/10.1016/S0040-1951\(99\)00078-5](https://doi.org/10.1016/S0040-1951(99)00078-5)
- Makropoulos KC, Burton PW (1985) Seismic hazard in Greece. II Ground Acceleration *Tectonophysics* 117:259–294. [https://doi.org/10.1016/0040-1951\(85\)90274-4](https://doi.org/10.1016/0040-1951(85)90274-4)
- Makropoulos K, Kaviris G, Kouskouna V (2012) An updated and extended earthquake catalogue for Greece and adjacent areas since 1900. *Nat Hazard* 12:1425–1430. <https://doi.org/10.5194/nhess-12-1425-2012>
- Marzocchi W, Taroni M (2014) Some thoughts on declustering in probabilistic seismic-hazard analysis. *Bull Seismol Soc Am* 104:1838–1845. <https://doi.org/10.1785/0120130300>
- Marzocchi W, Taroni M, Selva J (2015) Accounting for Epistemic Uncertainty in PSHA: Logic Tree and Ensemble Modeling. *Bull Seismol Soc Am* 105:2151–2159. <https://doi.org/10.1785/0120140131>
- Mavroulis S, Lekkas E (2021) Revisiting the most destructive earthquake sequence in the recent history of Greece: Environmental Effects Induced by the 9, 11 and 12 August 1953 Ionian Sea Earthquakes. *Appl Sci* 11:8429. <https://doi.org/10.3390/app11188429>
- McGuire RK (1976) FORTRAN computer program for seismic risk analysis (Report No. 76–67), Open-File Report. <https://doi.org/10.3133/ofr7667>
- McKay D, Beckman R, Conover W (1979) A Comparison of three methods for selecting values of input variables in the analysis of output from a computer code. *Technometrics* 21:239–245. <https://doi.org/10.2307/1268522>
- McKenzie D (1972) Active Tectonics of the Mediterranean Region. *Geophys J R Astron Soc* 30:109–185. <https://doi.org/10.1111/j.1365-246X.1972.tb02351.x>
- Pagani M, Monelli D, Weatherill G, Danciu L, Crowley H, Silva V, Henshaw P, Butler L, Nastasi M, Panzeri L, Simonato M, Vigano D (2014) OpenQuake Engine: An open hazard (and Risk) Software for the Global Earthquake Model. *Seismol Res Lett* 85:692–702. <https://doi.org/10.1785/0220130087>
- Papadimitriou P, Kaviris G, Makropoulos K (2006) The Mw = 6.3 2003 Lefkada Earthquake (Greece) and induced stress transfer changes. *Tectonophysics* 423:73–82. <https://doi.org/10.1016/j.tecto.2006.03.003>
- Papadimitriou E, Karakostas V, Mesimeri M, Chouliaras G, Kourouklas C (2017) The Mw6.5 17 November 2015 Lefkada (Greece) Earthquake: Structural Interpretation by Means of the Aftershock Analysis. *Pure Appl Geophys* 174:3869–3888. <https://doi.org/10.1007/s00024-017-1601-3>
- Papadimitriou P, Kapetanidis V, Karakonstantis A, Spingos I, Pavlou K, Kaviris G, Kassaras I, Sakkas V, Voulgaris N (2021) The 25 October, 2018 Zakynthos (Greece) earthquake: seismic activity at the transition between a transform fault and a subduction zone. *Geophys J Int* 225:15–36. <https://doi.org/10.1093/gji/ggaa575>
- Papadimitriou P, Voulgaris N, Kouskouna V, Kassaras I, Kaviris G, Pavlou K, Karakonstantis A, Bozionelos G, Kapetanidis V (2014) The Kefallinia Island earthquake sequence January–February 2014. In Proceedings of the Second European Conference on Earthquake Engineering and Seismology (2ECEES), Istanbul, Turkey, 24–29 August 2014
- Papadimitriou P (1988) Etude de la structure du manteau supérieur de l'Europe et modélisation des ondes de volume engendrées par des séismes Egeens, PhD thesis. University of Paris, Paris
- Papazachos BC, Papaioannou CA, Papazachos CA, Savvaidis AS (1999) Rupture zones in the Aegean region. *Tectonophysics* 308:205–221. [https://doi.org/10.1016/S0040-1951\(99\)00073-6](https://doi.org/10.1016/S0040-1951(99)00073-6)
- Papazachos BC, Papazachou CB (2003) The Earthquakes of Greece. Ziti Publications, Thessaloniki, p 273. (In Greek)

- Pavlou K, Kaviris G, Kouskouna V, Sakkas G, Zymvragakis A, Sakkas V, Drakatos G (2021) Minor seismic hazard changes in the broader area of Pournari artificial lake after the first filling (W. Greece). *Results Geophys Sci* 100025. <https://doi.org/10.1016/j.ringsps.2021.100025>
- Pérouse E, Sébrier M, Braucher R, Chamot-Rooke N, Bourlès D, Briole P, Sorel D, Dimitrov D, Arsenikos S (2017) Transition from collision to subduction in Western Greece: the Katouna-Stamna active fault system and regional kinematics. *Int J Earth Sci* 106:967–989. <https://doi.org/10.1007/s00531-016-1345-9>
- Pirazzoli SC, PA, Laborel J, Laborel-Deguen F (1994) The 1953 earthquake in Cephalonia (Western Hellenic Arc): coastal uplift and halotectonic faulting. *Geophys J Int* 117: 834–849. <https://doi.org/10.1111/j.1365-246X.1994.tb02474.x>
- Robson DS, Whitlock JH (1964) Estimation of a truncation point. *Biometrika* 51:33–39. <https://doi.org/10.1093/biomet/51.1-2.33>
- Sachpazi M, Hirn A, Clément C, Haslinger F, Laigle M, Kissling E, Charvis P, Hello Y, Lépine J-C, Sapin M, Ansorge J (2000) Western Hellenic subduction and Cephalonia Transform: Local earthquakes and plate transport and strain. *Tectonophysics* 319:301–319. [https://doi.org/10.1016/S0040-1951\(99\)00300-5](https://doi.org/10.1016/S0040-1951(99)00300-5)
- Sakkas V, Lagios E (2015) Fault modelling of the early-2014 ~M6 Earthquakes in Cephalonia Island (W. Greece) based on GPS measurements. *Tectonophysics* 644–645:184–196. <https://doi.org/10.1016/j.tecto.2015.01.010>
- Sakkas G, Kouskouna V, Makropoulos K (2010) Seismic hazard analysis in the Ionian Islands using macroseismic intensities. *Hell J Geosci* 45:239–248
- Sakkas V, Kapetanidis V, Kaviris G, Spingos I, Mavroulis S, Diakakis M, Alexopoulos JD, Kazantzidou-Firtinidou D, Kassaras I, Dilalos S, Vassilakis E, Kotsi E, Tselentis G, Lekkas E, Voulgaris N (2022) Seismological and ground deformation study of the ionian islands (W. Greece) during 2014–2018, a Period of Intense Seismic Activity. *App Sci* 12. <https://doi.org/10.3390/app12052331>
- Sakkas G (2016) Calculation and analysis of the seismic motion rotational components in Greece, Ph.D. Thesis. Geophysics-Geothermics Department, Faculty of Geology, University of Athens, Greece (in Greek). 278. <https://doi.org/10.12681/eadd/39773>
- Scordilis EM, Karakaisis GF, Karacostas BG, Panagiotopoulos DG, Comninakis PE, Papazachos BC (1985) Evidence for transform faulting in the Ionian sea: The Cephalonia island earthquake sequence of 1983. *Pure Appl Geophys PAGEOPH* 123:388–397. <https://doi.org/10.1007/BF00880738>
- Skarlatoudis AA, Papazachos CB, Margaritis BN, Theodulidis N, Papaioannou Ch, Kalogeras I, Scordilis EM, Karakostas V (2007) Erratum to empirical peak ground-motion predictive relations for shallow earthquakes in Greece. *Bull Seismol Soc Am* 97:2219–2221. <https://doi.org/10.1785/0120070176>
- Skarlatoudis AA, Papazachos CB, Margaritis BN, Theodulidis N, Papaioannou CH, Kalogeras I, Scordilis EM, Karakostas V (2003) Empirical peak ground-motion predictive relations for shallow earthquakes in Greece. *Bullet Seismologic Soc Am* 93:2591–2603. <https://doi.org/10.1785/0120030016Stiros>
- Sokos E, Kiratzi A, Gallovič F, Zahradník J, Serpetsidaki A, Plicka V, Janský J, Kostelecký J, Tselentis GA (2015) Rupture process of the 2014 Cephalonia, Greece, earthquake doublet (Mw6) as inferred from regional and local seismic data. *Tectonophysics* 656:131–141. <https://doi.org/10.1016/j.tecto.2015.06.013>
- Stiros SC, Pirazzoli PA, Laborel J, Laborel-Deguen F (1994) The 1953 earthquake in Cephalonia (Western Hellenic Arc): coastal uplift and halotectonic faulting. *Geophys J Int* 117:834–849. <https://doi.org/10.1111/j.1365-246X.1994.tb02474.x>
- Stucchi M, Rovida A, Gomez Capera AA, Alexandre P, Camelbeeck T, Demircioglu MB, Gasperini P, Kouskouna V, Musson RMW, Radulian M, Sesetyan K, Vilanova S, Baumont D, Bungum H, Fäh D, Lenhardt W, Makropoulos K, Martinez Solares JM, Scotti O, Živčić M, Albini P, Batlo J, Papaioannou C, Tatevossian R, Locati M, Meletti C, Viganò D, Giardini D (2013) The SHARE European Earthquake Catalogue (SHEEC) 1000–1899. *J Seismol* 17:523–544. <https://doi.org/10.1007/s10950-012-9335-2>
- Taroni M, Akinci A (2021) Good practices in PSHA: declustering, b-value estimation, foreshocks and aftershocks inclusion; a case study in Italy. *Geophys J Int* 224:1174–1187. <https://doi.org/10.1093/gji/ggaa462>
- Underhill JR (1989) Late Cenozoic deformation of the Hellenide foreland, western Greece. *Geol Soc Am Bull* 101:613–634. [https://doi.org/10.1130/0016-7606\(1989\)101%3c0613:LCDOTH%3e2.3.CO;2](https://doi.org/10.1130/0016-7606(1989)101%3c0613:LCDOTH%3e2.3.CO;2)
- Valkaniotis S, Ganas A, Papanthassiou G, Papanikolaou M (2014) Field observations of geological effects triggered by the January–February 2014 Cephalonia (Ionian Sea, Greece) earthquakes. *Tectonophysics*. <https://doi.org/10.1016/j.tecto.2014.05.012>
- Wang Z (2005) A clear definition of seismic hazard and risk: A basis for hazard and risk assessment, communication, and management. Presented at the AGU Fall Meeting Abstracts, pp S53B–1110
- Wiemer S, Wyss M (2000) Minimum magnitude of completeness in earthquake catalogs: Examples from Alaska, the Western United States, and Japan. *Bull Seismol Soc Am* 90:859–869. <https://doi.org/10.1785/0119990114>
- Woessner J, Laurentiu D, Giardini D, Crowley H, Cotton F, Grünthal G, Valensise G, Arvidsson R, Basili R, Demircioglu MB, Hiemer S, Meletti C, Musson RW, Rovida AN, Sesetyan K, Stucchi M The SHARE Consortium (2015) The 2013 european seismic hazard model: key components and results. *Bull Earthq Eng* 13:3553–3596. <https://doi.org/10.1007/s10518-015-9795-1>
- Zhou Y, Zhou S, Zhuang J (2018) A test on methods for MC estimation based on earthquake catalog. *Earth Planet Phys* 2:150–162. <https://doi.org/10.26464/epp2018015>

Publisher's Note Springer Nature remains neutral with regard to jurisdictional claims in published maps and institutional affiliations.

Springer Nature or its licensor (e.g. a society or other partner) holds exclusive rights to this article under a publishing

agreement with the author(s) or other rightsholder(s); author self-archiving of the accepted manuscript version of this article

is solely governed by the terms of such publishing agreement and applicable law.